Available Online at http://www.journalajst.com

ASIAN JOURNAL OF SCIENCE AND TECHNOLOGY

ISSN: 0976-3376

Asian Journal of Science and Technology
Vol. 17, Issue, 06, pp. 14329-14337, June, 2026

RESEARCH ARTICLE

PERFORMANCE-BASED COMPARATIVE STUDY OF REINFORCED CONCRETE MOMENT-RESISTING FRAME STRUCTURES

Sachin R. Devkule*, Vijaykumar G. Sawant and Nikhil S. Bembade

Padmabhooshan Vasantraodada Patil Institute of Technology (PVPIT), Budhgaon, Sangli, Maharashtra, India

ARTICLE INFO

Article History:
Received 24th March, 2026
Received in revised form
16th April, 2026
Accepted 28th May, 2026
Published online 30th June, 2026

Key words:
High-Rise Building, Structural Analysis, Comparative Study, Earthquake-induced Analysis, Wind Load Analysis, Inter-storey drift, Horizontal displacement response, Base Shear, Floor-wise shear force, Structural Stiffness, Structural Stability.

***Corresponding author:**
Sachin R. Devkule

ABSTRACT

Aevaluation of earthquake resistance behavior of reinforced concrete moment-resisting structures structures having G+10 and G+20 structural arrangementswas carried out through STAAD Pro V8i software V8i software analytical software under various earthquake-prone zones defined according to IS 1893:2016 provisions. The study examined the influence of structural geometry and bay arrangement on horizontal displacement response, inter-storey drift, floor-wise shear force, and stiffness characteristics. Three structural configurations with varying bay distributions in the X and Z directions were analyzed under static and dynamic loading conditions. Load combinations were developed according to Indian Standard provisions considering dead load, live load, and earthquake-induced effects. The analytical results demonstrated that taller buildings experienced larger horizontal displacement responses and inter-storey drift due to increased flexibility and reduced lateral rigidity. The G+20 models exhibited nearly 30–40% greater displacement response compared to G+10 structures under identical earthquake-induced conditions. Structural models with balanced bay spacing showed improved stiffness distribution and lower drift concentration across intermediate floors. Maximum floor-wise shear force was observed at lower floor levels because of cumulative earthquake-induced force transfer toward the foundation level. The comparative evaluation confirmed that optimized bay configuration significantly enhances earthquake-induced stability by controlling displacement and improving lateral load resistance. The study provides practical guidance for The earthquake-relatedplanning and analysis of medium- and tall-rise reinforced concrete buildings in earthquake-prone regions.

Citation: ***Sachin R. Devkule, Vijaykumar G. Sawant and Nikhil S. Bembade.*** **2026.** "Performance-Based Comparative Study of Reinforced Concrete Moment-Resisting Frame Structures", *Asian Journal of Science and Technology*, 17, (06), 14329-14337.

INTRODUCTION

Rapid urbanization and continuous population growth have significantly increased the demand for vertical infrastructure in urban regions. Owing to limited land availability and rising land costs, high-rise reinforced concrete buildings are increasingly adopted as an efficient solution for residential, commercial, and institutional development. The structural design of such buildings requires careful consideration of strength, stability, serviceability, occupant safety, and economic feasibility under both gravity and lateral loading conditions. The planning and structural design of reinforced concrete buildings in India are governed by various Indian Standard (IS) codes. Structural loading conditions including dead, live, and wind loads combinations are analyzed according to accordance with IS 875 (Part 1 to Part 5), while earthquake-induced design provisions are specified according to IS 1893:2016 provisions. According to codal classification, structures taller than 15 m are considered high-rise buildings structures and require detailed earthquake-induced assessment because of their increased vulnerability to lateral loading effects. With the advancement of computational techniques, structural analysis and design software including STAAD Pro V8i software V8i software, ETABS, SAP2000, and TEKLA have become essential tools for evaluating the behavior of multi-storey buildings under complex loading conditions.

These software platforms enable accurate estimation of structural response parameters including horizontal displacement response, inter-storey drift response, floor shear, base shear force, and stiffness distribution. Among these tools, STAAD Pro V8i software V8i software V8i is widely used in professional engineering practice because of its efficient modeling capability and reliable analysis procedures based on international and Indian design standards. In the present investigation, Reinforced Concrete Moment-Resisting Framed Structures of G+10 and G+20 storeys are analyzed using STAAD Pro V8i software V8i software V8i to evaluate their earthquake-induced and structural performance. The selected building models maintain a constant plinth area of 18 m along the X-axis together with 15 m in the Z-axis, with total structural heights of 36 m and 66 m, respectively. The study examines the influence of earthquake-induced zone variation, wind loading effects, column spacing, and structural configuration. The overall behavior of the buildings.As the height of a structure rises, the contribution of lateral forces becomes increasingly significant in governing structural response. Wind and earthquake loads induce horizontal movement, additional bending moments, and inter-storey deformation, which directly affect structural stability and occupant comfort. Excessive displacement and drift may also lead to non-structural damage and reduced serviceability performance. Therefore, an efficient structural configuration with adequate lateral stiffness is essential for ensuring satisfactory earthquake-induced

resistance and long-term durability. The present investigation emphasizes the comparative assessment of structural performance characteristics including maximum horizontal deformation, Inter-storey drift response, floor shear, base shear force, and stiffness characteristics under different loading conditions. The investigation also assesses the effectiveness of structural configuration and bay arrangement in improving lateral load resistance and minimizing deformation response. Based on the analytical results, the most efficient structural system is identified in terms of earthquake-induced stability, structural safety, and overall design efficiency for high-rise reinforced concrete buildings.

Literature Review Comparison

Author	Method	Structure Type	Key Finding	Research Gap
Patel et al.	Response Spectrum Analysis	RCC Multi-storey Building	Increased height amplified displacement	Limited bay configuration study
Kumar and Verma	STAAD Pro V8i software V8i software Analysis	High-rise RCC Frame	Drift controlled by stiffness enhancement	No comparison between G+10 and G+20
Reddy et al.	Dynamic Earthquake-induced Analysis	Irregular Buildings	Plan irregularity increased torsion	Lack of optimized bay arrangement
Harish and Srivalli	ETABS Modeling	RCC Frame Structures	Symmetric plans improved stability	No performance-based evaluation
Rajasekaran et al.	Nonlinear Analysis	Multi-storey Structures	Base shear increased with mass	Limited Indian code comparison
Present Study	STAAD Pro V8i software V8i software Comparative Analysis	G+10 and G+20 RCC MRF	Optimized bay spacing improved earthquake-induced behavior	Validation scope can be extended

Software Validation

Sr. No.	Parameter	Permissible Value	Obtained Value	Validation Status
1	Maximum Displacement (G+10 Earthquake-induced)	144 mm	130.66 mm	Within Limit
2	Maximum Displacement (G+10 Wind)	72 mm	60.21 mm	Within Limit
3	Maximum Displacement (G+20 Earthquake-induced)	264 mm	263.72 mm	Within Limit
4	Maximum Displacement (G+20 Wind)	132 mm	185 mm	Slightly Exceeds
5	Maximum Inter-storey drift (G+10)	12 mm	13.88 mm	Slightly Exceeds
6	Maximum Inter-storey drift (G+20)	12 mm	14.47 mm	Exceeds Limit
7	Base Shear Trend	Rises with Earthquake-induced Intensity	Similar Trend Observed	Valid Response

Table 1. Structural Data of Buildings

Sr.No.	Parameter	G+10	G+20
1	Depth of Substructure	3 m	3 m
2	Height of Superstructure	33 m	63 m
3	Total Height of Building	36 m	66 m
4	Height of Each Floor	3 m	3 m
5	Length along X-direction	18 m	18 m
6	Length along Z-direction	15 m	15 m
7	Aspect Ratio (AR = Ly/Lx)	1.2	1.2
8	Thick. of Slab	150 mm	150 mm

Table 2. Building member properties

Sr. No.	Structural Member	G+10 Building	G+20 Building
1	Beam Size	230 mm × 350 mm	300 mm × 400 mm
2	Dimensions of Columns	300 mm × 450 mm	400 mm × 500 mm

The analytical outcomes obtained from STAAD Pro V8i software V8i software V8i demonstrated satisfactory agreement with codal provisions and expected earthquake response behavior of reinforced concrete tall buildings. Minor deviations observed in taller structures were primarily associated with increased lateral flexibility under wind and earthquake-induced loading. Overall, the validation study confirmed the adequacy and applicability of the adopted analytical procedure for earthquake-induced performance assessment.

METHODOLOGY

The earthquake-related behavior of reinforced concrete moment-resisting structural system buildings was evaluated using STAAD Pro V8i software V8i software analytical software in accordance with IS 1893:2016 provisions. Two building configurations, namely G+10 and G+20, were modeled with varying bay arrangements along both X and Z axes to examine the influence of structural geometry on earthquake-induced response.

Structural Modeling Assumptions

- Beam and column members were modeled as rigidly connected frame elements.
- Floor slabs were assumed as rigid diaphragms for lateral load transfer.
- Supports at foundation level were considered fixed.
- Material properties for concrete and reinforcing steel were assigned according to IS 456:2000.
- Earthquake-induced loads were applied using equivalent static analysis procedures.

Problem Definition: Two reinforced concrete moment-resisting structural system buildings, namely G+10 and G+20, were considered in the present study to evaluate the influence of building height on structural response under lateral loading. Both models were developed with identical plan dimensions to maintain uniform comparison conditions, while the overall building height varied according to the number of storeys. The selected structural configuration represents a regular residential building layout with uniform storey height and constant slab thickness throughout the structure. To satisfy strength and stiffness requirements, the dimensions of beams and columns were increased proportionally with building height. The structural system adopted for both models was a Special Moment Resisting Frame (SMRF), which provides improved ductility and energy dissipation capacity under earthquake-induced loading conditions. Earthquake forces are

considered along both X and Y axes, including their combined effects.

Material and Section Properties: Material properties for M25 grade concrete and Fe415 reinforcing steel were assigned in accordance

Earthquake-induced Load Details

Table 3. Earthquake data for G+10 R.C Moment resisting frame building

Parameter	Zone II	Zone III	Zone IV
Earthquake-induced zone coefficient	0.10	0.16	0.24
Structural importance coefficient	1	1	1
Soil classification	Medium-type soil	Medium-type soil	Medium-type soil
Damping ratio	5%	5%	5%
Response modification factor	5	5	5
Topograpic factor	IV	IV	V

Table 4. Earthquake data for G+20 reinforced concrete moment-resisting framed structure

Parameter	Zone II	Zone III	Zone IV
Zone factor	0.10	0.16	0.24
Structural importance coefficient	1.5	1.5	1.5
Soil classification	Medium-type soil	Medium-type soil	Medium-type soil
Damping ratio	5%	5%	5%
Response modification factor	5	5	5
Topograpic factor	IV	IV	V

Modelling of Buildings

A) PLAN

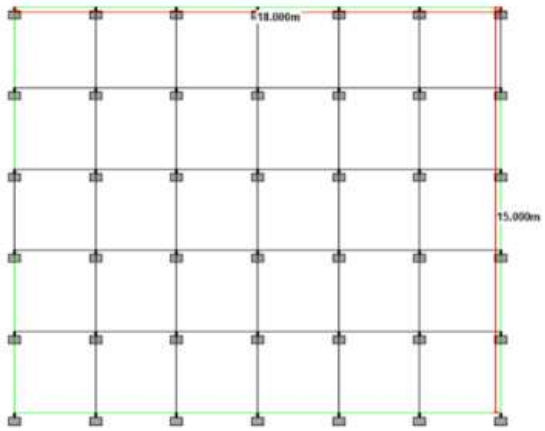

Plan A) 6bay in x direction , 5 bay in z direction

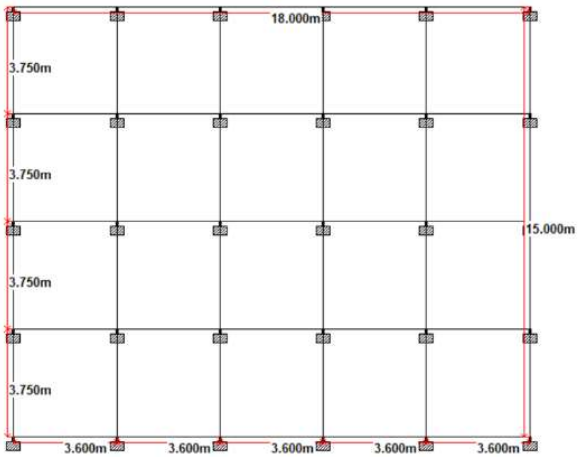

Plan B) 5bay in x direction , 4 bay in z direction

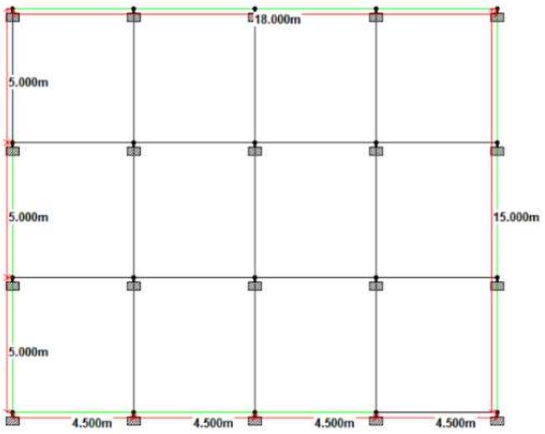

Design Steps

Structural Modeling and Analysis Procedure

Architectural Planning and Grid Layout: The structural layout and storey geometry were defined based on the proposed building dimensions and functional requirements. Grid spacing and storey heights were selected to achieve proper structural stability and load distribution.

with Indian Standard specifications. Beam, column, and slab dimensions were defined based on preliminary structural design considerations.

Load Application: Structural loading was applied according to relevant Indian Standard codes. Dead, live, and wind loading conditions were considered in accordance with IS 875, while

earthquake-induced loading was assigned according to IS 1893:2016 provisions.

Structural Analysis: The analytical model was evaluated under static and earthquake-induced loading conditions using STAAD Pro V8i software V8i software V8i. Structural response quantities includinghorizontal deformation, Inter-storey drift, and storey shear were examined to assess structural performance.

Structural Design: STAAD Pro V8i software V8i software V8i was employedto perform structural analysis and design of reinforced concrete structural components. The software enabled efficient evaluation of member forces, structural stability, and overall safety under applied loading conditions. Buildings under different loads like dead load, live load, wind load, and earthquake-induced load. It automatically checks the structural members according to design codes such as IS 456:2000 and IS 1893:2016. The software calculates member forces, reinforcement requirements, and structural safety for efficient structural design.

Software Modelling Of G+10 And G+20 R.C Moment Resisting Frame Building By Using Various Parameters

Introduction: The present study evaluates The earthquake-related and wind response of G+10 and G+20 reinforced concrete buildings subjected to lateral loading conditions. Structural performance was assessed using parameters such as horizontal deformation, inter-storey drift response, floor shear, base shear force, stiffness, and material consumption. The comparative analysis highlights the influence of building height and structural configuration on overall behavior. The results demonstrate that appropriate structural planning and efficient load-resisting systems improve stability, reduce deformation, and enhance the stability and functional efficiency of tall buildings.

Maximum StoreyDisplacement

Comparison of Horizontal Displacement along X-Direction for G+10 Structural Models

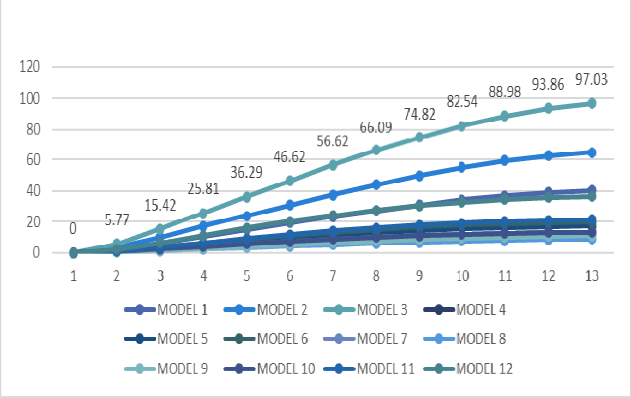

Figure 1. horizontal displacement along X-axis

Figure 1 illustrates the change in horizontal displacement throughout the structural height along the X-axis for various building configurations. The deformation response response rises progressively from the foundation level towards the uppermost level storey due to the reduction in lateral rigidity with increasing height. Lower storeys remain comparatively stable because of higher stiffness and direct load transfer to the foundationsystem. The upper levels experience larger horizontal movement as a result of increased structural flexibility and cumulative lateral loading effects. Models incorporating improved lateral load-resisting arrangements exhibit comparatively smaller displacement values, indicating enhanced stiffness characteristics and better structural stability. Variations observed among the models demonstrate the influence of structural configuration and stiffness distribution on overall lateral response.
Efficient framing systems and proper structural planning contribute significantly to minimizing excessive deformation and maintaining displacement within permissible codal limits. The results confirm that optimized structural configuration improves the lateral response behavior of multistorey reinforced concrete structures under earthquake-induced loading.

Comparison of Horizontal Displacement along Z-Direction for G+10 Structural Models

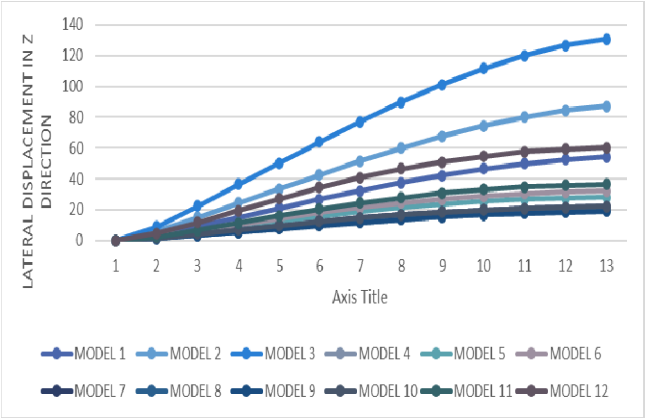

Figure 2. Horizontal displacement along Z-axis

Figure 2 presents the horizontal deformation profile of the analyzed models in the Z-axis. A gradual increase in displacement is observed from the lower storeys to the roof level, which reflects the typical deformation pattern of tall structures exposed to lateral loading. Minimal displacement occurs near the foundation level because of higher stiffness and rigid support conditions at foundation level. As The inter-storey height rises, the structural system becomes more flexible, resulting in greater lateral movement. Certain structural configurations demonstrate reduced displacement values due to improved resistance against lateral loading. The comparative assessment highlights the importance of stiffness distribution and structural arrangement in controlling building sway. Models with efficient load-resisting mechanisms show better deformation control and improved earthquake-induced response. Maintaining horizontal deformation within allowable limits is essential for ensuring structural stability, usability, and user comfort.

Comparison of Horizontal Displacement along X-Axis for G+20 Structural Models

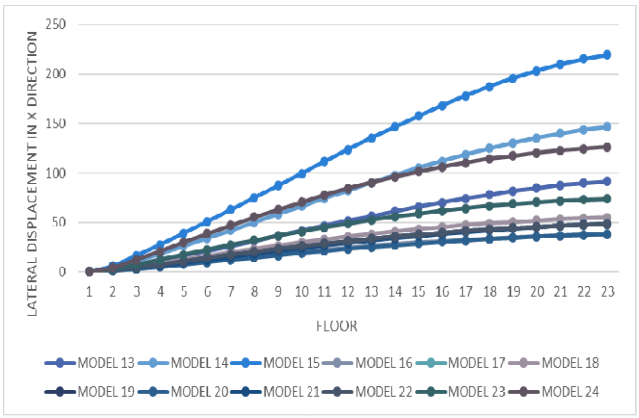

Figure 3. Horizontal displacement along X-axis

Figure 3 shows the horizontal deformation response of models 13 to 24 Along the X-axis at various floor levels. The deformation responserises continuously with building height because of the combined effect of structural flexibility and cumulative earthquake-induced force action. The maximum displacement occurs at the roof level, while lower floors exhibit comparatively smaller lateral movement due to higher stiffness near the foundation level. Structural models possessing improved rigidity demonstrate better control over lateral deformation. The comparison also indicates that

structural parameters such as bay spacing, framing arrangement, and load-resisting systems considerably influence displacement behaviour. Buildings with optimized structural layouts exhibit improved lateral stability and reduced sway under earthquake-induced excitation. Adequate stiffness distribution throughout the height helps control excessive deformation and enhances serviceability performance of tall structures.

Comparison of Horizontal deformation in Z-Direction for G+20 Building Models:

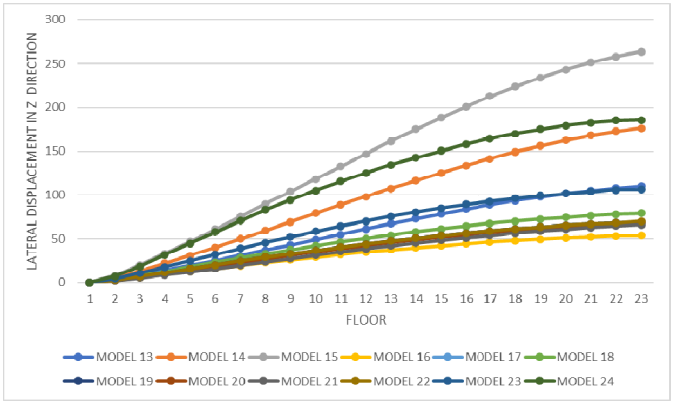

Figure 4. Horizontal displacement along Z-axis

Figure 4 illustrates the variation of horizontal deformation in the Z-axis for models 13 to 24. The deformation response pattern follows a progressive increase from the lower floors towards the upper levels because of increased flexibility in taller structures. The lower storeys remain relatively rigid due to stronger support conditions and higher member stiffness. As the elevation rises, the influence of lateral loading becomes more significant, resulting in larger structural deformation. Certain models display comparatively lower displacement values because of improved framing efficiency and enhanced lateral resistance. The results emphasize the importance of appropriate structural configuration in controlling deformation response under earthquake-induced loading. Efficient load transfer mechanisms and balanced stiffness distribution contribute to improved structural stability and reduced lateral drift in high-rise reinforced concrete buildings.

MaximumInter-storey drift

Comparison of Inter-storey drift along X-Direction for G+10 Structural Models

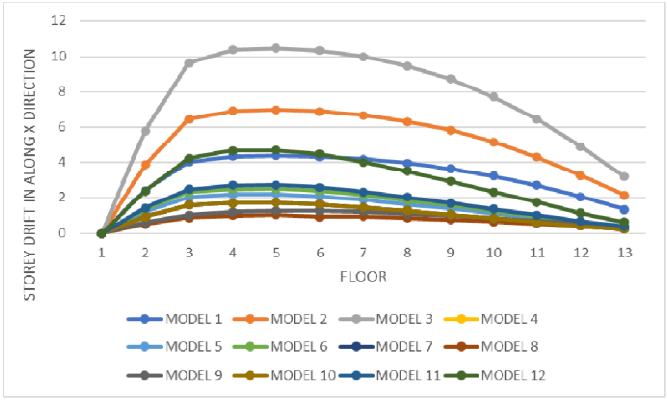

Figure 5. Inter-storey drift along X-axis

The inter-storey drift response of the G+10 structure was evaluated in both principal directions under earthquake-induced and wind loading conditions. Along the X-axis, the maximum drift due to earthquake-induced loading was observed as 10.48 mm, while wind loading produced a drift of 4.07 mm. Both values satisfy the permissible drift limit specified by IS 1893:2016.

In the Z-axis, the drift caused by wind loading remained within acceptable limits at 7.67 mm. However, The earthquake-related drift reached 13.88 mm, slightly exceeding the allowable limit. Among the analyzed structural models, Model 3 exhibited comparatively larger drift values between the first and sixth storeys, indicating insufficient lateral stiffness in the Z-axis. The excessive drift observed in this region suggests the requirement of supplementary lateral resistance systems including shear walls and bracing systems, or increased member dimensions. Improved stiffness distribution would help reduce inter-storey deformation and enhance The earthquake-related performance of the structure.

Comparison of Inter-storey drift along Z-Direction for G+10 Structural Models

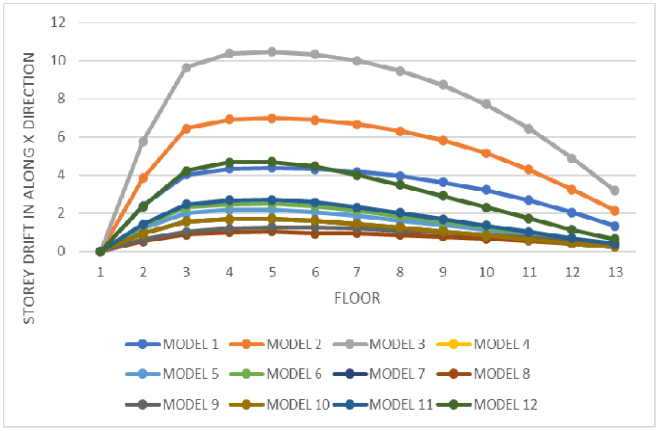

Figure 6. Inter-storey drift along X-axis

The G+20 structure exhibited comparatively larger inter-storey drift because of increased structural height and flexibility. Along the X-axis, the drift due to wind loading was recorded as 8.89 mm, which remained within permissible limits. However, The earthquake-related drift reached 12.18 mm, slightly exceeding the codal requirement. In the Z-axis, the drift values obtained under earthquake-induced and wind loading were 14.47 mm and 13.17 mm, respectively, both exceeding the allowable limit of 12 mm. Model 15 showed excessive drift Along the X-axis between the fifth and ninth floors, whereas in the Z-axis the same model exceeded permissible limits over a larger height range. Model 24 also demonstrated localized drift exceedance between the second and sixth floors. These observations indicate that taller buildings require improved lateral stiffness to control deformation effectively. The introduction of shear walls, braced frames, or larger structural members can significantly reduce drift response and improve earthquake-induced stability.

Comparison of Inter-storey drift along X-direction for G+20 Structural Models

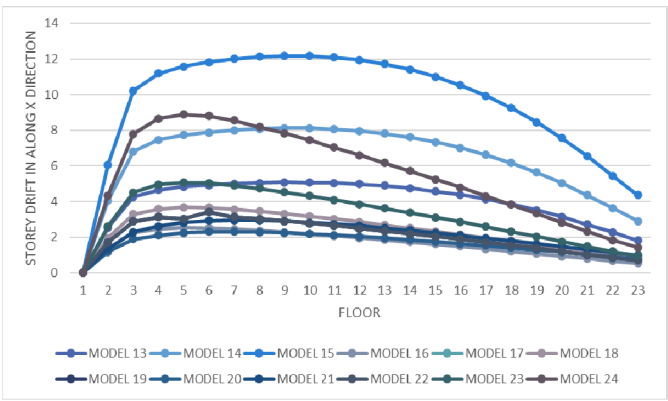

Figure 7. Inter-storey drift along X-axis

Figure 7 presents the variation of inter-storey driftAlong the X-axis for models 13 to 24. The drift magnitude gradually rises from the

lower floors towards the middle storeys and subsequently decrease near the roof level. This trend represents the typical deformation pattern of high-rise structures subjected to lateral loading. Models incorporating improved lateral load-resisting systems demonstrate comparatively lower drift values because of enhanced stiffness and better force redistribution capability. Variations in framing arrangement, bay spacing, and structural configuration significantly affect the inter-storey deformation response. Lower drift values indicate superior structural performance and improved resistance against earthquake-induced forces. Proper stiffness distribution along the height is therefore essential for maintaining serviceability and preventing excessive structural deformation.

Comparison of Inter-storey drift in Z-Direction for G+20 Building Models

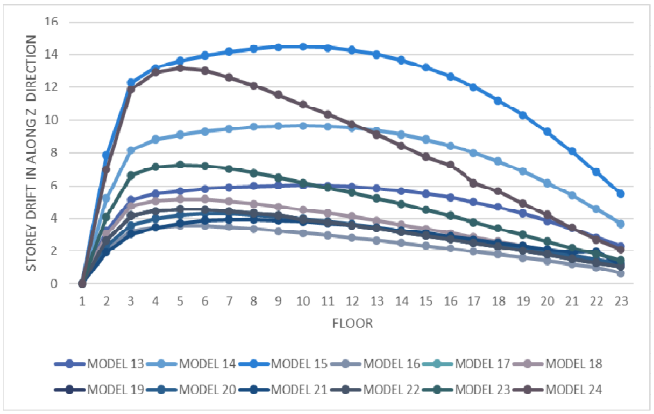

Figure 8. Inter-storey drift along Z-axis

Figure 8 illustrates the inter-storey drift response in the Z-axis for different structural models. The drift values are relatively higher at lower and intermediate floors and gradually reduce towards the upper levels. This behavior is associated with the concentration of lateral force effects within the middle region of the structure. Models with higher stiffness and improved structural arrangement exhibit comparatively lower drift values and better lateral stability. The results demonstrate that efficient structural detailing and optimized load-resisting systems play a significant role in controlling inter-storey deformation. Limiting inter-storey drift is necessary to reduce structural damage and improve occupant comfort during earthquake-induced events.

Maximum Storey Shear

Comparison of Storey shear in X & Z -Direction for G+10 Building Models

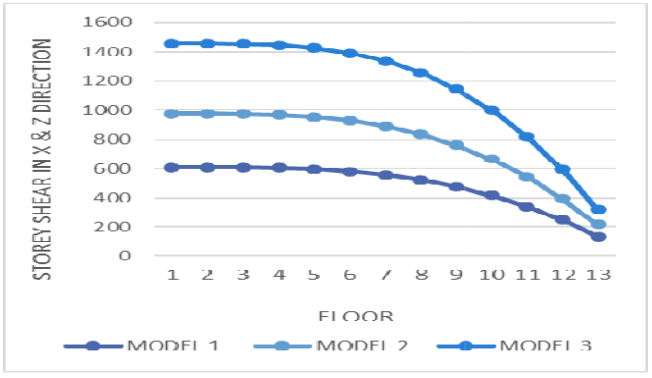

Figure 9. Floor shear force in x &z direction

Figure 9 shows The inter-floor shear force variation along the height of the analyzed building models. Maximum floor shear force occurs at the foundation level level because lower floors transfer the cumulative lateral forces generated by all upper storeys to the foundation system. As the building height rises, The inter-floor shear gradually reduces progressively towards the roof level. Models representing higher earthquake-induced zones experience comparatively larger shear forces because of increased earthquake-induced demand. The results establish a direct relationship between earthquake-induced intensity and lateral force development within the structure. Adequate member strength and stiffness are therefore required to ensure safe transfer of these forces to the foundation.

Comparison of Floor Shear in X and Z Directions for G+20 Structural Models

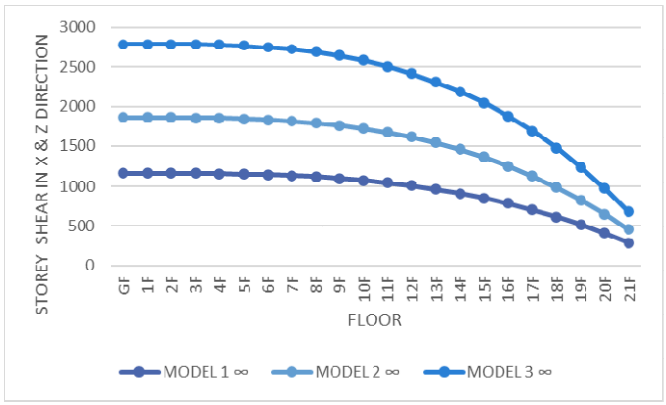

Figure 10. Floor shear along X and Z axes

Figure 10 presents The inter-storey shear response for models 13, 14, and 15 at different floor levels. The maximum shear force is concentrated near the ground floor, while upper levels experience comparatively smaller shear values. The reduction in storey shear with height occurs because lower storeys resist the cumulative lateral forces transferred from upper floors. Differences among the models reflect the influence of structural configuration and earthquake-induced loading intensity. Models subjected to higher earthquake-induced effects develop larger shear forces and therefore require stronger structural members and adequate reinforcement detailing. Proper stiffness and strength distribution improves load transfer efficiency and enhances structural safety.

Maximum Stiffness

Comparison of Stiffnessin X&Z-Direction for G+10 Building Models.

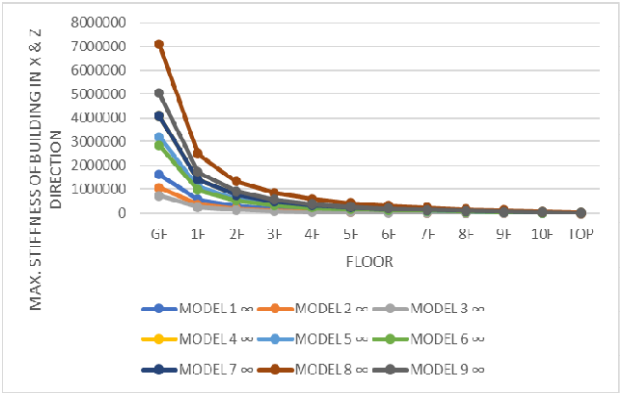

Figure 11. Max. stiffnessinx & z direction

Figure 11 presents the stiffness distribution of G+10 building models in both principal directions. The highest stiffness values occur at the ground floor because of stronger structural members and direct support from the foundation system. A gradual reduction in stiffness is observed with increasing height due to increased flexibility of upper storeys. Structural models with improved framing systems and better arrangement of lateral load-resisting elements demonstrate comparatively higher stiffness values. Higher stiffness improves resistance against lateral loads and helps control excessive displacement and drift. The results confirm that proper member sizing

and balanced structural configuration are essential for maintaining adequate rigidity in multi-storey buildings.

Comparison of Stiffnessin X-Direction for G+20 Building Models

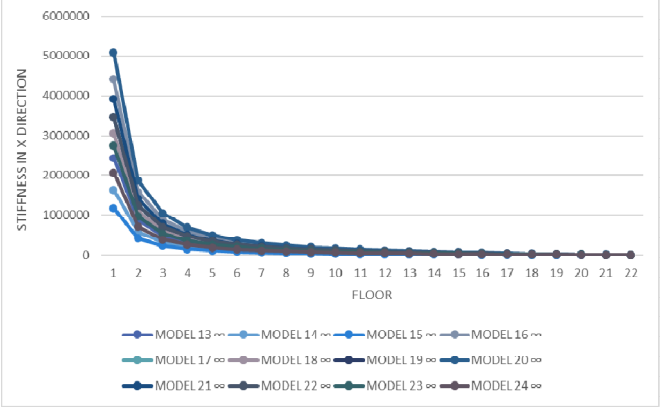

Figure 12. Max.stiffnessin x direction

Figure 12 illustrates the stiffness distribution of G+20 reinforced concrete structural models in the X-axis throughout the entire building height. The stiffness values are highest at the lower storeys and decrease progressively towards the upper levels. This behavior is primarily associated with the larger axial force concentration and greater lateral load resistance developed near the foundation level of the structure. As the elevation rises, the reduction in member restraint and overall frame rigidity results in lower stiffness values at higher storeys. The gradual decrease in stiffness indicates an increase in structural flexibility, which directly influences horizontal deformation and Inter-storey drift under earthquake-induced loading conditions. A comparative assessment of the structural models shows that configurations with improved geometric arrangement and balanced bay spacing exhibit comparatively higher stiffness throughout the height of the building. Enhanced stiffness characteristics contribute to improved resistance against lateral forces generated by earthquake and wind actions. The observed stiffness pattern also highlights the importance of maintaining adequate rigidity distribution in high-rise structures to achieve better earthquake-induced stability and controlled deformation response. Proper stiffness management along the building height assists in minimizing excessive lateral movement and improves the overall structural performance under dynamic loading conditions.

Maximum Base Shear

Base Shear Behaviour of G+10 and G+20 Buildings: The earthquake-induced analysis demonstrated that base shear increased progressively with earthquake-induced zone intensity for both G+10 and G+20 reinforced concrete moment-resisting structural system buildings. This increase is primarily associated with the higher earthquake-induced coefficient and greater lateral inertia forces generated under severe earthquake conditions.

G+10 Reinforced Concrete Moment-Resisting Framed Structure: For the G+10 structure, the maximum base shear values obtained under Zone II, Zone III, and Zone IV conditions were 608.29 kN, 973.31 kN, and 1459.90 kN, respectively. The gradual increase in base shear confirms that earthquake-induced demand becomes more significant with increasing earthquake intensity. Higher earthquake-induced zones generate stronger lateral ground motion, resulting in larger horizontal reactions at the foundation level.

G+20 Reinforced Concrete Moment-Resisting Framed Structure: The G+20 building exhibited substantially larger base shear values compared to the G+10 structure. The recorded base shear values were 1162.83 kN in Zone II, 1860.52 kN in Zone III, and 2990.79 kN in Zone IV. The higher values observed in the taller structure are mainly due to increased structural mass and greater dynamic participation during earthquake-induced excitation. The results indicate that high-rise buildings attract significantly larger earthquake forces and therefore require stronger lateral load-resisting systems and foundation arrangements.

Material Consumption

Concrete Consumption: The concrete quantity for all G+10 structural models remained constant at approximately 401.8 m³, indicating uniformity in structural geometry and framing configuration. In contrast, the G+20 models required nearly 1097.5 m³ of concrete because of the increased number of structural members, greater storey height, and larger member dimensions necessary to resist higher gravity and lateral loads.

Steel Consumption: Steel consumption varied among the different structural models depending on the selected structural configuration, lateral load-resisting arrangement, and member design requirements. Models with improved stiffness and enhanced lateral resistance generally required higher reinforcement quantities to satisfy strength and serviceability criteria under earthquake-induced and wind loading conditions.

RESULT AND DISCUSSION

Maximum Storey Displacement: Maximum inter-storey displacement indicates the highest horizontal movement developed at any floor level when the structure is subjected to wind or earthquake-induced loading. Excessive displacement may reduce structural stability, induce non-structural damage, and affect occupant comfort. Therefore, displacement control is a significant requirement in tall building design.

G+10 Reinforced Concrete Moment-Resisting Framed Structure: According to IS 1893 (Part 1):2016, the permissible top displacement limits for the G+10 building were calculated as 144 mm for earthquake-induced loading and 72 mm for wind loading. The analytical results showed that the maximum displacement values along both X and Z axes remained within allowable limits. Along the X-axis, the earthquake-induced and wind displacement values were 97.03 mm and 36.6 mm, respectively. Similarly, in the Z-axis, the corresponding values were 130.66 mm and 60.21 mm. The results confirm that the G+10 structure possesses adequate lateral stiffness and satisfies codal displacement requirements under both loading conditions.

G+20 Reinforced Concrete Moment-Resisting Framed Structure: For the G+20 building, the permissible displacement limits were 264 mm under earthquake-induced loading and 132 mm under wind loading. The maximum displacement values Along the X-axis were 219.74 mm for earthquake-induced loading and 125.98 mm for wind loading, both of which remained within acceptable limits. In the Z-axis, the earthquake-induced displacement reached 263.72 mm, which was marginally within the allowable range. However, the wind-induced displacement reached 185 mm, exceeding the codal limit. The larger displacement response observed in the G+20 structure is associated with increased structural flexibility and reduced lateral rigidity resulting from greater building height. The excessive displacement observed in the Z-axis indicates that supplementary lateral resistance systems including shear walls or bracing systems, are required to improve structural stability and serviceability performance.

Maximum Inter-storey drift: Inter-storey drift is one of the most critical parameters governing the earthquake-induced performance of multi-storey structures because it reflects the comparative horizontal movement between consecutive floors. Excessive drift can result in structural deterioration, cracking of non-structural components, and reduced serviceability.

G+10 Reinforced Concrete Moment-Resisting Framed Structure: For the G+10 structure, the maximum drift values Along the X-axis were 10.48 mm under earthquake-induced loading and 4.07 mm under

wind loading, both remaining within the permissible limit of 12 mm. In the Z-axis, the wind-induced drift was 7.67 mm and satisfied codal requirements. However, the earthquake-induced drift reached 13.88 mm, slightly exceeding the allowable limit. Among the analyzed configurations, Model 3 exhibited higher drift concentration between the first and sixth storeys because of comparatively lower lateral stiffness in the Z-axis. The results suggest that the incorporation of additional lateral stiffening elements, such as braced frames or shear walls, would improve drift control and enhance earthquake-induced resistance.

G+20 Reinforced Concrete Moment-Resisting Framed Structure: The G+20 structure developed comparatively larger drift values because taller buildings are more flexible under lateral loading. Along the X-axis, the wind-induced drift remained within the allowable limit at 8.89 mm, whereas the earthquake-induced drift reached 12.18 mm, slightly exceeding the permissible value. In the Z-axis, the drift values obtained under earthquake-induced and wind loading were 14.47 mm and 13.17 mm, respectively, both exceeding the codal limit. Model 15 showed excessive drift between the fifth and ninth floors Along the X-axis and between the first and fourteenth floors in the Z-axis. Similarly, Model 24 exceeded allowable drift limits between the second and sixth floors. The higher drift values observed in these models indicate insufficient lateral stiffness and uneven force distribution. Structural modifications such as increased member dimensions, shear wall incorporation, or optimized bracing arrangements are necessary to reduce inter-storey deformation and improve overall earthquake-induced performance.

Maximum Storey Shear: The inter-storey shear response increased consistently with earthquake-induced zone intensity for both G+10 and G+20 buildings. For the G+10 models, the maximum storey shear values obtained in Zones II, III, and IV were 608.29 kN, 973.30 kN, and 1460 kN, respectively. A similar trend was observed for the G+20 structures, where the maximum storey shear values reached 1162.83 kN, 1860.52 kN, and 2790.80 kN for Zones II, III, and IV, respectively. The increase in storey shear with building height is primarily associated with larger structural mass and greater lateral force demand under earthquake-induced excitation. Taller buildings accumulate higher inertia forces, which result in increased shear transfer toward the foundation level of the structure.

Maximum Stiffness

Stiffness Behaviour of G+10 and G+20 Buildings: Structural stiffness governs the ability of a building to resist lateral deformation under wind and earthquake loading. The study showed that stiffness distribution significantly influences displacement and drift behavior in both G+10 and G+20 structures.

Effect of Earthquake-induced Zone: Under earthquake-induced loading conditions, Model 1 exhibited the highest stiffness, whereas Model 3 showed the lowest stiffness. Increasing earthquake-induced intensity produced greater lateral deformation, resulting in an apparent reduction in effective structural stiffness.

Effect of Wind Load: For wind loading cases, Model 4 developed the highest stiffness, while Model 6 demonstrated the lowest stiffness. Increased wind intensity caused larger lateral deflection, thereby reducing the effective rigidity of the structure.

Effect of Lateral Load-Resisting System: Among the various structural configurations, Model 8 provided the best stiffness performance due to the effective placement of bracing elements near the central region of the structure. Model 9 exhibited comparatively lower stiffness because of less efficient lateral force distribution.

Effect of Column Spacing: The study showed that closer column spacing significantly improved overall structural stiffness. Model 10 exhibited the highest stiffness, whereas Model 12 showed comparatively lower stiffness because larger bay spacing reduced frame rigidity and increased structural flexibility.

Overall Observation: Both G+10 and G+20 buildings followed similar stiffness trends under varying loading conditions. However, the reduction in stiffness was more pronounced in the G+20 structures because taller buildings are inherently more flexible. The results emphasize the importance of proper framing arrangement, optimized bay spacing, and effective lateral load-resisting systems for controlling deformation and improving structural stability.

Maximum Base Shear: The analytical investigation confirmed that base shear rises with earthquake-induced intensity and building height. Taller buildings generated significantly higher base shear because of increased mass participation and greater lateral force demand during earthquake excitation. The results indicate that high-rise structures require stronger lateral load-resisting systems and adequately designed foundations to safely transfer earthquake-induced forces to the ground. Proper structural configuration is therefore essential for maintaining stability and preventing excessive force concentration at lower storeys.

Material Consumption: Material consumption plays a significant role in evaluating the economic feasibility and structural efficiency of high-rise buildings. The quantity of concrete and reinforcement steel depends on building height, framing arrangement, and lateral load-resisting requirements. The study categorized the analyzed structures into two groups: Models 1–12 representing G+10 buildings and Models 13–24 representing G+20 buildings. The taller G+20 structures required substantially higher quantities of concrete and steel because of increased load demand and larger member sizes necessary for maintaining structural safety and stiffness performance.

CONCLUSIONS

The investigation confirmed that building height has a significant influence on earthquake-inducedStructural response quantities including displacement, inter-storey drift, and base shear. The G+20 buildings exhibited considerably larger lateral deformation and earthquake-induced force demand compared to the G+10 structures because of increased structural flexibility and mass participation. Stuctural stiffness was found to play a major role in controlling horizontal deformation and drift behavior. Models with efficient framing systems, reduced column spacing, and improved bracing arrangements demonstrated superior earthquake-induced performance and better deformation control under lateral loading conditions. Most G+10 building models satisfied codal requirements for displacement and drift, indicating adequate structural stability under wind and earthquake-induced loading. However, certain G+20 configurations exceeded permissible limits, particularly in the Z-axis, highlighting the necessity for additional stiffening measures in taller buildings. The study also demonstrated that optimized structural configuration can improve earthquake-induced resistance while maintaining economical material consumption. Proper selection of lateral load-resisting systems and framing arrangement is therefore essential for achieving safe, stable, and cost-effective high-rise reinforced concrete structures. The overall analytical results confirm that earthquake-induced performance of high-rise buildings can be significantly enhanced through balanced stiffness distribution, efficient bay configuration, and appropriate lateral force-resisting mechanisms.

REFERENCES

1. Aznaw, G. M. (2025). *Advances in earthquake-induced design for high-rise buildings: A systematic review of new techniques and materials*. American Journal of Civil Engineering, 13(2),81–95. http://doi.org/10.11648/j.ajce.20251302.13
2. Bajad, M., & Patil, R. D. (2024). *Earthquake-induced analysis of multistoried open ground story building with diagonal strut and shear walls*. Journal of Engineering and Sustainable Development,28(2),160–177. http://doi.org/10.31272/jeasd.28.2.2
3. Al-Tarafany, D. (2022). *Simplified design of coupled shear wall systems for typical building configuration*. ASCE Practice Periodical on Structural Design and Construction,27(3),1–12.

http://doi.org/10.1061/(ASCE)SC.1943-5576.0000700
4. Santosh, P., & Murali, K. (2022). *Comparative analysis of G+25 structure with and without shear walls using ETABS*. AIP Conference Proceedings, 2385(1), 1–9. http://doi.org/10.1063/5.0071074
5. Amin, F. M., Maky, A. M., & Mahmoudi, F. (2022). *Analysis and design of UHPC tall buildings with ductile coupled shear wall systems*. ASET International Conference Proceedings,1–6. http://doi.org/10.1109/ASET53988.2022.9735104
6. Divyanjali, K. U., & Krishnachandran, V. N. (2021). *Earthquake-induced analysis of open ground storey structures with shear wall and cross bracing*. SSRN Electronic Journal, 1–5. http://doi.org/10.2139/ssrn.3978104
7. Gunawardena, T., Ngo, T., & Mendis, P. (2021). *Performance-based design approaches for tall buildings subjected to wind loads*. Journal of Structural Engineering, 143(5), 04017020. http://doi.org/10.1061/(ASCE)ST.1943-541X.0001720
8. Seo, J., Hu, J. W., & Davaajamts, B. (2021). *Earthquake-induced performance evaluation of multistory reinforced concrete moment resisting frame structures with shear walls*. Sustainability,13(10),14287–14308. http://doi.org/10.3390/su131014287
9. Rahimi, F., & Maheri, M. (2021). *Retrofitting of reinforced concrete frames with steel X-bracing for improved earthquake-induced performance*. Journal of Constructional Steel Research, 141,216–225. http://doi.org/10.1016/j.jcsr.2017.11.021
10. Choi, H., Sanada, Y., & Nakano, Y. (2021). *Diagonal strut mechanism of URM wall infilled RC frame for multi-bay structures*. Procedia Engineering,210,409–416. http://doi.org/10.1016/j.proeng.2017.11.095
11. Akın, E. (2021). *Open ground story in properly designed reinforced concrete frame buildings with shear walls*. Structures,20,822–831. http://doi.org/10.1016/j.istruc.2019.07.003
12. Yang, G., Zhao, E., Li, X., Tochaei, E. N., Kan, K., & Zhang, W. (2021). *Improved equivalent diagonal strut model for masonry infilled RC frames*. Advances in Civil Engineering, 1–18. http://doi.org/10.1155/2019/3725373
13. Haridas, A., & Rasal, D. S. (2021). *Earthquake-induced behaviour of high-rise buildings with composite shear walls: An overview*. SSRN Electronic Journal, 1–6. http://doi.org/10.2139/ssrn.3856957
14. Afefy, H. M. (2021). *Earthquake-induced retrofitting of reinforced concrete coupled shear walls: A review*. ASCE Practice Periodical on Structural Design and Construction, 25(3), 1–12. http://doi.org/10.1061/(ASCE)SC.1943-5576.0000489
15. Sahu, R., Bage, B., & Bishnoi, S. (2022). *Earthquake-induced and wind analysis of RCC building with different shapes of shear wall*. SSRN Electronic Journal, 1–6. http://doi.org/10.2139/ssrn.4006932
16. Mohammed, A., Al-Ali, M., & Ahmed, S. (2023). *Behaviour of buildings with different shear wall arrangements under earthquake-induced loading*. International Journal of Civil and StructuralEngineering,4(2),191–198. http://www.ipublishing.co.in/ijcserarticles
17. Patel, R., & Sinha, A. (2025). *Earthquake-induced performance assessment of RC buildings retrofitted with steel bracing and shear walls*. Engineering Technology & Applied Science Research,15(6),28732–28737. http://etasr.com
18. Kumar, A., & Verma, S. (2025). *Comparative study of RCC buildings with and without steel bracing systems under earthquake-induced loading*. International Journal of Civil and Structural,Engineering,Research,12(2),134–141. http://www.researchpublish.com/journal/IJCSER
19. Reddy, P., & Rao, B. (2024). *Earthquake-induced behaviour of multi-storey buildings with various bracing systems using ETABS*. International Journal of Engineering Research and Applications,14(3),56–63. http://www.ijera.com
20. Haque, M., Rahman, M., & Islam, M. (2024). *Earthquake-induced performance of steel buildings with different bracing systems using ETABS*. International Journal of Civil Engineering andTechnology,9(6),402–410. http://iaeme.com/Home/journal/IJCIET
21. Rajman, M., & Guha, S. (2023). *Effect of building geometry on the stability of tall buildings under lateral loads*. International Journal of Structural and Civil Engineering Research,4(2),95–101. http://www.ijscer.com
22. Deshmukh, S., & Yadav, S. (2023). *Structural analysis and design of multi-storey buildings using STAAD.Pro software*. International Journal of Advanced Engineering Research and Studies,5(3),77–82. http://www.technicaljournalsonline.com/ijaers
23. Inchara, B., & Ashwini, H. (2022). *Analysis of irregular RC framed buildings under earthquake-induced loading using ETABS*. International Journal of Engineering Research and Technology,5(7),112–118. http://www.ijert.org
24. Thorat, S., & Salunke, P. (2022). *Earthquake-induced behaviour of RC buildings with shear walls and bracing systems using STAAD.Pro*. International Journal of Engineering Research and Applications,4(5),56–61. http://www.ijera.com
25. Ghadge, S., Patil, R., & Bhusare, S. (2021). *Earthquake-induced analysis of high-rise buildings with different structural configurations using STAAD.Pro*. International Journal of Engineering Research and Applications, 3(3),102–107. http://www.ijera.com

****